2020 7th International Conference on Control, Decision and
Information Technologies (CoDIT'20) | Prague, Czech Republic / June 29 - July 2, 2020

Special Cases in the Attitude Determination of Three-Vehicle Heterogeneous Formations

Pedro Cruz[1] and Pedro Batista[2]

***Abstract*— This paper considers the attitude determination problem of a three-vehicle heterogeneous formation, whose line of sight is constrained. By some reason, such as large distance, two of the vehicles, the deputies, cannot measure the direction of each other's position. The deputies can only measure the relative direction relative to the chief, which is the remaining vehicle in the formation. The special cases of the problem are described in terms of the number of solutions related to each configuration. In general, there is only one solution, but infinite or even two ambiguous solutions are possible, respectively in the degenerate and ambiguous configurations. These arise due to lack of information or symmetry in the data, respectively. Furthermore, the subset of special configurations is a zero measure set of the global set of configurations, which is an important property of the problem. Simulations that test and validate the described configurations are shown as well, which also help to understand what effects the quality of the solution obtained according to a special case proximity metric.**

I. INTRODUCTION

Attitude determination is the computation of the angular relation between different frames in a given moment, usually between two vehicle frames or between a vehicle frame and an inertial frame. It is an important aspect of any navigation system and critical to many applications. The development of this field of study was propelled by the dawn of spaceflight. In that period, fundamental methods were designed including the Tri-Axial Attitude Determination (TRIAD) algorithm [1] and Wahba's optimization problem was formulated [2], which is an alternative formulation of the Orthogonal Procrustes problem, both well recognized in the field. Later, several methods for solving that optimization problem were proposed, such as the Davenport's q-method [3], the Quaternion Estimator (QUEST) method [4], which uses the quaternion representation of the attitude, and the Singular Value Decomposition (SVD) decomposition based methods [5], to name only a few. A more recent example is the Fast Linear Quaternion Attitude Estimator (FLAE) [6], which can reduce the computational time while having similar accuracy to other methods, and many others exist.

The work of P. Cruz was supported by the PhD Grant PD/BD/143143/2019 from FCT. This work was also supported by the Fundação para a Ciência e a Tecnologia (FCT) through LARSyS - FCT Project UIDB/50009/2020 and through the FCT project DECENTER [LISBOA-01-0145-FEDER-029605], funded by the Programa Operacional Regional de Lisboa 2020 and PIDDAC programs.

The authors are with the Institute for Systems and Robotics, Laboratory for Robotics and Engineering Systems, Portugal. The authors are also with the Department of Electrical and Computer Enginerring, Instituto Superior Técnico, Universidade de Lisboa, Portugal.

[1]pfcruz@isr.tecnico.ulisboa.pt

[2]pbatista@isr.tecnico.ulisboa.pt

Attitude determination methods rely on sensor measurements. Relative direction sensors such as focal plane arrays of complementary metal-oxide semiconductor (CMOS) pixels, as those used in star trackers [7], are of interest for many applications, specially when relative navigation is necessary. This kind of sensor can measure the direction to different sections of other vehicles. Nonetheless, if there is considerable noise, for instance, because the vehicle is far away, then the average direction to the vehicle as a whole can be measured instead. An advantage of these sensors is the ability to operate in Global Positioning System (GPS) denied environments, such as the interplanetary space or the interior of buildings.

Vehicle formations have been gaining attention for some time now [8], for their potential to accomplish the same mission with relatively simpler systems, with increased reliability and redundancy. These advantages are particularly attractive for space applications which have, generally, high costs and risks. Also in the field of cooperative mobile robots, where formations are included, there is interest in heterogeneous groups, which are defined by having non-identical individual elements [9]. That is the context of the formation considered in this paper, which is called an heterogeneous formation, because different vehicles have different sets of navigation sensors, namely with respect to the line-of-sight sensing capacity. Other problems with some similarities include [10] and [11].

Multi-spacecraft observatories located further from Earth can be used to synthesize large aperture telescopes or long baseline interferometers or even to sample spatially disperse phenomena such as the Earth's magnetotail [12]. Another idea is to use a small spacecraft formation as an orbiting antenna for interplanetary communication, for instance between Earth and Mars, which would then relay the data to ground stations.

The main contribution of this paper is the description of the configurations in which the solution to the attitude determination problem in [13] is not unique. These cases include the degenerate cases, where insufficient data leads to an infinite number of solutions and also the ambiguous cases where symmetries in the information gathered by the sensors results in two different solutions.

This work is divided as follows: first the problem and respective solution are described. In the following section, a description of the degenerate and ambiguous cases is given. Also in this section, the importance of the measure of the subset of special configurations being zero is discussed. The third section, shows the simulation results of the problem as

978-1-7281-5953-9/20/$31.00 ©2020 IEEE

the configurations get closer to a degenerate or an ambiguous situation. Finally, some remarks are made in the conclusion about these results and future work.

II. PROBLEM AND SOLUTION

A. Notation

Throughout this document, scalars are represented in regular typeface, whereas vectors and matrices are represented in bold, with the latter in capital case. The symbol $\mathbf{I}$ represents the identity matrix with the appropriate dimensions. The four-quadrant inverse tangent function is denoted by $\mathrm{atan2}\,(b,a)$, with $a,b \in \mathbb{R}$. The set of unit vectors in $\mathbb{R}^3$ is denoted by $S(2) := \left\{\mathbf{x} \in \mathbb{R}^3 : \|\mathbf{x}\| = 1\right\}$. The special orthogonal group of dimension 3, which describes proper rotations, is denoted by $SO(3) := \{\mathbf{X} \in \mathbb{R}^{3\times 3} : \mathbf{X}\mathbf{X}^T = \mathbf{X}^T\mathbf{X} = \mathbf{I} \ \wedge \ \det(\mathbf{X}) = 1\}$. The skew-symmetric matrix parameterized by $\mathbf{x} \in \mathbb{R}^3$, which encodes the cross product between $\mathbf{x}$ and another vector, is denoted by

$$\mathbf{S}(\mathbf{x}) := \begin{bmatrix} 0 & -x_3 & x_2 \\ x_3 & 0 & -x_1 \\ -x_2 & x_1 & 0 \end{bmatrix}, \ \mathbf{x} = \begin{bmatrix} x_1 \\ x_2 \\ x_3 \end{bmatrix}.$$

The rotation matrix in $SO(3)$ that transforms a given vector, in $\mathbb{R}^3$, expressed in the body-fixed frame of vehicle i to the body-fixed frame of vehicle j, $i,j \in \mathbb{N}_0$, is denoted by $\mathbf{R}_i^j$. In the case of rotations to and from the inertial frame, the letter I is used instead of the vehicle number. Moreover, multiple candidates for the same rotation are identified by a subscript capital case letter, such as $\left(\mathbf{R}_i^j\right)_A$. The rotation matrix of an angle $\theta \in \mathbb{R}$ around the axis described by the unit vector $\mathbf{x} \in$ S(2) is denoted by $\mathbf{R}(\theta, \mathbf{x})$, which is written as [7]

$$\mathbf{R}(\theta,\mathbf{x}) := \cos(\theta)\,\mathbf{I} + (1-\cos(\theta))\mathbf{x}\,\mathbf{x}^T - \sin(\theta)\,\mathbf{S}(x) \ .$$

B. Problem Statement

Consider a three-vehicle formation, whose vehicles are equipped with sensors capable of measuring the direction to other vehicles in the line of sight, such as focal plane arrays, and sensors that can measure inertial direction vectors, such as star trackers or magnetometers. The value of the latter are known *a priori* in the earth-centered inertial frame, for example, from celestial maps. In this formation, two of the vehicles cannot measure each other's relative position, either because they are too distant from one another or from the characteristics of their sensor set. These two vehicles are the deputies, also referred as vehicles 2 and 3, and the vehicle without line of sight constraints is called the chief or simply vehicle 1. Moreover, every vehicle can measure one inertial direction individually, hence each vehicle can use a different sensor to obtain this measurement, which emphasizes the heterogeneity of the formation.

The line of sight measurement of vehicle 2 taken by the chief in its own body fixed frame is denoted as $\mathbf{d}_{1/2}$, analogously there are three other measurements, namely $\mathbf{d}_{2/1}$, $\mathbf{d}_{1/3}$, and $\mathbf{d}_{3/1}$. The inertial measurements are taken in the respective body frames and denoted as $\mathbf{d}_1$, $\mathbf{d}_2$, and $\mathbf{d}_3$. The respective representations in the inertial frame are known *a priori* and are denoted, respectively, by ${}^I\mathbf{d}_1$, ${}^I\mathbf{d}_2$, and ${}^I\mathbf{d}_3$. The formation and respective measurements are depicted in Fig. 1.

The goal of the problem is to find all relative $\left(\mathbf{R}_2^1, \mathbf{R}_3^1, \mathbf{R}_3^2\right)$ and inertial attitudes $\left(\mathbf{R}_1^I, \mathbf{R}_2^I, \mathbf{R}_3^I\right)$.

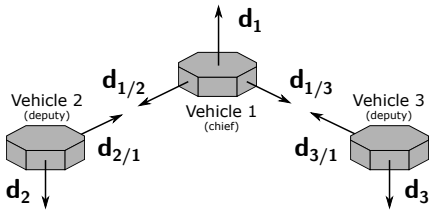

Fig. 1. Three-vehicle heterogeneous formation

A scenario where this problem could be applied is a three spacecraft interferometer, where the distance between two of the vehicles makes a bearing measurement between them impossible.

C. Solution

The solution that follows is a summary of the algorithm detailed in [13]. It consists in finding candidates for the same attitude, in this case $\mathbf{R}_1^I$, supported by different data. For that matter, consider a branch as the sub-formation that consists of the chief and a deputy, along with the respective inertial and line of sight measurements, as depicted in Fig. 2 for the case with vehicle 2.

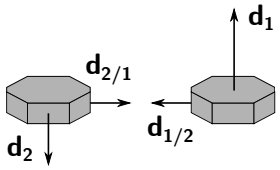

Fig. 2. Branch 1-2 of the formation

In this formation, there are two branches, respectively referred as 1-2 or 1-3, according to which deputy is considered. There are four possible candidates for $\mathbf{R}_1^I$, two from each branch. Since the attitude is independent of which branch's data were used, then at least one candidate in branch 1-2 is identical to a candidate in branch 1-3. The solution set results from these identical candidates. As will be described in the next section, this process gives, in general, a single solution.

In the following description, consider only branch 1-2. The results for branch 1-3 are analogous and thus not shown here.

1) Relative Attitude: In order to find $\mathbf{R}_1^I$ with branch 1-2, compute first the relative attitude $\mathbf{R}_2^1$. For that matter consider the relations of the branch measurements given by

$$-\mathbf{d}_{1/2} = \mathbf{R}_2^1\mathbf{d}_{2/1} \tag{1}$$

and

$${}^I\mathbf{d}_1^T\,{}^I\mathbf{d}_2 = \mathbf{d}_1^T\mathbf{R}_2^1\mathbf{d}_2 \ . \tag{2}$$

Then, decompose $\mathbf{R}_2^1$ into a product of two rotations, parameterized by an angle and a unit length axis, as follows

$$\mathbf{R}_2^1 := \mathbf{R}\left(\theta_2, \mathbf{n}_2\right)\mathbf{R}\left(\theta_1, \mathbf{n}_1\right) \ . \tag{3}$$

The parameters of (3), such that both (1) and (2) are satisfied, are given by

$$\theta_1 := \pi \ ,$$

$$\begin{cases} \mathbf{n}_1 := \frac{\mathbf{d}_{2/1}-\mathbf{d}_{1/2}}{\|\mathbf{d}_{2/1}-\mathbf{d}_{1/2}\|} & , \text{ for } \mathbf{d}_{2/1} \neq \mathbf{d}_{1/2} \\ \mathbf{n}_1 := \frac{\mathbf{S}\left(\mathbf{d}_{1/2}\right)\mathbf{d}_1}{\|\mathbf{S}\left(\mathbf{d}_{1/2}\right)\mathbf{d}_1\|} & , \text{ for } \mathbf{d}_{2/1} = \mathbf{d}_{1/2} \end{cases} ,$$

$$\theta_2 := \operatorname{atan2}\left(a_{s_{12}}, a_{c_{12}}\right) \pm \arccos\left(\frac{a_{p_{12}}}{\sqrt{a_{s_{12}}^2 + a_{c_{12}}^2}}\right) \ , \tag{5a}$$

and

$$\mathbf{n}_2 := -\mathbf{d}_{1/2} \ ,$$

with

$$\begin{cases} a_{p_{12}} & := \mathbf{d}_1^T(\mathbf{d}_{1/2})(\mathbf{d}_{1/2})^T\mathbf{d}_2^* - {}^I\mathbf{d}_1^T \ {}^I\mathbf{d}_2 \\ a_{c_{12}} & := \mathbf{d}_1^T\mathbf{S}\left(\mathbf{d}_{1/2}\right)^2\mathbf{d}_2^* \\ a_{s_{12}} & := \mathbf{d}_1^T\mathbf{S}\left(-\mathbf{d}_{1/2}\right)\mathbf{d}_2^* \end{cases} ,$$

where

$$\mathbf{d}_2^* := \mathbf{R}\left(\theta_1, \mathbf{n}_1\right)\mathbf{d}_2 \ .$$

Notice that (5a) has two solutions in general, therefore, this method results in two candidates, $\left(\mathbf{R}_2^1\right)_A$ and $\left(\mathbf{R}_2^1\right)_B$.

2) Inertial Attitude: Next, compute the candidates $\left(\mathbf{R}_1^I\right)_A$ and $\left(\mathbf{R}_1^I\right)_B$, from the branch's relations given by

$${}^I\mathbf{d}_1 = \mathbf{R}_1^I\mathbf{d}_1$$

and

$${}^I\mathbf{d}_2 = \mathbf{R}_1^I\mathbf{R}_2^1\mathbf{d}_2 \ .$$

These relations can be solved with the TRIAD algorithm [14] which results in

$$\left(\mathbf{R}_1^I\right)_A = {}^I\mathbf{d}_1\mathbf{d}_1^T + \left(\frac{\mathbf{S}\left({}^I\mathbf{d}_1\right){}^I\mathbf{d}_2}{\|\mathbf{S}\left({}^I\mathbf{d}_1\right){}^I\mathbf{d}_2\|}\right)\left(\frac{\mathbf{S}\left(\mathbf{d}_1\right)\left(\mathbf{R}_2^1\right)_A\mathbf{d}_2}{\|\mathbf{S}\left(\mathbf{d}_1\right)\left(\mathbf{R}_2^1\right)_A\mathbf{d}_2\|}\right)^T + \left(\mathbf{S}\left({}^I\mathbf{d}_1\right)\frac{\mathbf{S}\left({}^I\mathbf{d}_1\right){}^I\mathbf{d}_2}{\|\mathbf{S}\left({}^I\mathbf{d}_1\right){}^I\mathbf{d}_2\|}\right)\left(\mathbf{S}\left(\mathbf{d}_1\right)\frac{\mathbf{S}\left(\mathbf{d}_1\right)\left(\mathbf{R}_2^1\right)_A\mathbf{d}_2}{\|\mathbf{S}\left(\mathbf{d}_1\right)\left(\mathbf{R}_2^1\right)_A\mathbf{d}_2\|}\right)^T$$

or

$$\left(\mathbf{R}_1^I\right)_B = {}^I\mathbf{d}_1\mathbf{d}_1^T + \left(\frac{\mathbf{S}\left({}^I\mathbf{d}_1\right){}^I\mathbf{d}_2}{\|\mathbf{S}\left({}^I\mathbf{d}_1\right){}^I\mathbf{d}_2\|}\right)\left(\frac{\mathbf{S}\left(\mathbf{d}_1\right)\left(\mathbf{R}_2^1\right)_B\mathbf{d}_2}{\|\mathbf{S}\left(\mathbf{d}_1\right)\left(\mathbf{R}_2^1\right)_B\mathbf{d}_2\|}\right)^T + \left(\mathbf{S}\left({}^I\mathbf{d}_1\right)\frac{\mathbf{S}\left({}^I\mathbf{d}_1\right){}^I\mathbf{d}_2}{\|\mathbf{S}\left({}^I\mathbf{d}_1\right){}^I\mathbf{d}_2\|}\right)\left(\mathbf{S}\left(\mathbf{d}_1\right)\frac{\mathbf{S}\left(\mathbf{d}_1\right)\left(\mathbf{R}_2^1\right)_B\mathbf{d}_2}{\|\mathbf{S}\left(\mathbf{d}_1\right)\left(\mathbf{R}_2^1\right)_B\mathbf{d}_2\|}\right)^T ,$$

according to the relative candidate used.

3) Comparison: After computing $\left(\mathbf{R}_1^I\right)_A$ and $\left(\mathbf{R}_1^I\right)_B$ from branch 1-2, and $\left(\mathbf{R}_1^I\right)_C$ and $\left(\mathbf{R}_1^I\right)_D$ from branch 1-3, compare the candidates from different branches. In the noiseless case, by construction, one of the following conditions is verified: i)$\left(\mathbf{R}_1^I\right)_A = \left(\mathbf{R}_1^I\right)_C$; ii)$\left(\mathbf{R}_1^I\right)_B = \left(\mathbf{R}_1^I\right)_C$; iii)$\left(\mathbf{R}_1^I\right)_A = \left(\mathbf{R}_1^I\right)_D$; and iv)$\left(\mathbf{R}_1^I\right)_B = \left(\mathbf{R}_1^I\right)_D$.

For that purpose, use the parameter that evaluates how close two rotation matrices are to each other, given by

$$\phi := \left|\arccos\left(\frac{\operatorname{trace}\left[\left(\mathbf{R}_1^I\right)_X\left(\mathbf{R}_1^I\right)_Y^T\right]-1}{2}\right)\right| \ ,$$

where $\left(\mathbf{R}_1^I\right)_X$ and $\left(\mathbf{R}_1^I\right)_Y$ represent two different candidates. This parameter is zero when both candidates are equal, which enables the disambiguation. In the presence of noise, the pair of candidates with the lowest value of ϕ are averaged using the SVD of the sum of both candidates. The result is the solution for $\mathbf{R}_1^I$. Moreover, the relative candidates that supported the computation of these inertial candidates also belong to the solution set.

4) Complete Solution: Finally, compute the remaining rotation matrices, with $\mathbf{R}_2^1$, $\mathbf{R}_3^1$, and $\mathbf{R}_1^I$, using the relations given by $\mathbf{R}_3^2 = \mathbf{R}_2^{1T}\mathbf{R}_3^1$, $\mathbf{R}_2^I = \mathbf{R}_1^I\mathbf{R}_2^1$, and $\mathbf{R}_3^I = \mathbf{R}_1^I\mathbf{R}_3^1$.

III. Special Cases

This section describes the special cases in which the problem laid out in the previous section has more than one solution. There are two kinds of such cases: the degenerate configurations which result in infinite solutions and the ambiguous configurations which result in two distinct solutions. All the remaining configurations have a unique solution.

The special configurations are expressed in the sequel, however, their proofs are not presented in this work due to the lack of space to elaborate on the technical details appropriately.

The major difference between both special cases is that, in the degenerate configurations, the solution accuracy will decrease as it gets closer to such cases, because the quality of the data is gradually decreasing. On the other hand, in the ambiguous configurations, the algorithm will suddenly output a different result, alternating between the two solutions, as the sensors' noise makes one or the other solution seem correct.

A. Degenerate Cases

The degenerate cases exist because there can be less data available than required, when two sensors measure parallel vectors. Hence, the problem becomes underdetermined, thus resulting in infinite solutions.

The degenerate cases can be divided according to the branch of the formation and the step of the solution. First, consider the branch 1-2 and the computation of candidates for the relative attitude, $\mathbf{R}_2^1$. There are infinite solutions when either of the following conditions is verified:

$$\begin{matrix} \mathbf{d}_{1/2} = \pm\mathbf{d}_1 \ ; \\ \mathbf{d}_{2/1} = \pm\mathbf{d}_2 \ . \end{matrix}$$

Next, consider the same branch and the computation of candidates for the inertial attitude, $\mathbf{R}_1^I$. There are infinite solutions when the following condition is verified:

$$ {}^I\mathbf{d}_1 = \pm\, {}^I\mathbf{d}_2 \ . $$

The degenerate conditions for the branch 1-3 are analogous to the previous three and respectively given by

$$ \begin{aligned} \mathbf{d}_{1/3} &= \pm\mathbf{d}_1 \ ; \\ \mathbf{d}_{3/1} &= \pm\mathbf{d}_3 \ ; \\ {}^I\mathbf{d}_1 &= \pm\, {}^I\mathbf{d}_3 \ . \end{aligned} \tag{6} $$

All these degenerate cases have only one relation involving the attitude that is being computed. Thus, one degree of freedom cannot be determined, which means there is a subset with infinite rotations that satisfy that relation.

B. Ambiguous Cases

The ambiguous cases are a consequence of the symmetries that characterize this problem. If the data in both branches are symmetric, then two indistinguishable solutions are possible, because the two candidates for $\mathbf{R}_1^I$ from branch 1-2 are the same as the two candidates from branch 1-3.

Intuitively, the configuration where the three vehicles are aligned, $\mathbf{d}_{1/2} = \pm\mathbf{d}_{1/3}$, and the inertial reference vectors of the deputies are identical, ${}^I\mathbf{d}_2 = \pm\, {}^I\mathbf{d}_3$, is an ambiguous case. Depicted in Fig. 3, the data in this configuration is symmetric, since both branches provide the same information.

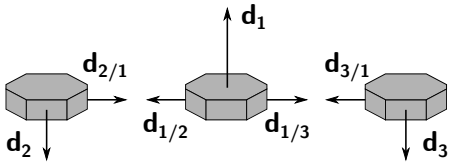

Fig. 3. Symmetric formation.

More symmetric configurations exist, nonetheless, they can all be derived from the previous configuration. All the ambiguous configurations must verify simultaneously the two conditions given by

$$ {}^I\mathbf{d}_2 = \mathbf{R}\left(\alpha,\, {}^I\mathbf{d}_1\right) \mathbf{R}\left(\beta, \frac{\mathbf{S}\left({}^I\mathbf{d}_1\right)\, {}^I\mathbf{d}_3}{\left\|\mathbf{S}\left({}^I\mathbf{d}_1\right)\, {}^I\mathbf{d}_3\right\|}\right)\, {}^I\mathbf{d}_3 \tag{7} $$

and

$$ \mathbf{d}_{1/2} = \mathbf{R}\left(\alpha, \mathbf{d}_1\right) \mathbf{R}\left(\gamma, \frac{\mathbf{S}\left(\mathbf{d}_1\right)\mathbf{d}_{1/3}}{\left\|\mathbf{S}\left(\mathbf{d}_1\right)\mathbf{d}_{1/3}\right\|}\right) \mathbf{d}_{1/3} \ , \tag{8} $$

where $\alpha,\ \beta,\ \gamma \in \mathbb{R}^3$. The marked areas in Figs. 4, 5, and 6 illustrate the effect of each angle of the conditions (7) and (8). These depictions help to understand what is the set of configurations with data symmetry.

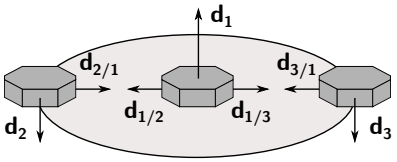

Fig. 4. Effect of α.

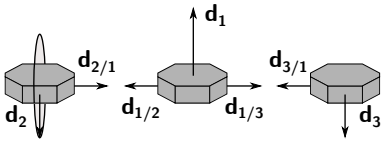

Fig. 5. Effect of β.

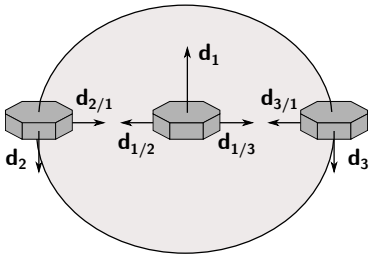

Fig. 6. Effect of γ.

C. Special cases measure

An important characteristic of the special configurations subset is that it is a zero measure subset of the configuration set. Hence, the probability of a configuration being exactly degenerate or ambiguous is zero. However, the accuracy is influenced by the proximity to these configurations and noise can make the solution jump between two attitudes in the ambiguous case, as discussed before. This property allows the problem to be applied in practical situations, with some care when getting close to such configurations.

IV. Simulation

In this section, a degenerate and an ambiguous case are simulated to demonstrate the previous conclusions. For simplicity and due to space limitations, only one of the degenerate configurations is simulated, because the results for the remaining configurations can be shown to be similar. The degenerate case chosen verifies (6) and the ambiguous case verifies both (7) and (8).

Both the degenerate and ambiguous cases were tested analyzing the error standard deviation evolution as the configuration approximates the respective special case. Close to the respective special cases, the standard deviation is expected to increase as the configuration gets close to a degenerate configuration. In contrast, when it gets close enough to an ambiguous configuration for the noise to alternate the outcome of the solution, it is expected to change suddenly, since the algorithm will choose only one attitude.

A. Sensor model

At each trial, random noise is added to each measurement taken by the sensors, following the QUEST model [15], because the sensor axes are assumed to be aligned with the

measurements. Therefore, denoting the image-space observation by the vector $\mathbf{m} \equiv [\chi\ \psi]^T$, its measurement model is given by $\tilde{\mathbf{m}} = \mathbf{m} + \mathbf{n}$ where $\tilde{\mathbf{m}}$ is the measurement and $\mathbf{n}$ is the noise. The noise model describing the uncertainty of the image-space observations is assumed to follow a zero mean Gaussian distribution, $\mathbf{n} \sim \mathcal{N}(\mathbf{0}, R_{\text{FOCAL}})$, with the covariance of the focal plane given by [15]

$$R_{\text{FOCAL}} = \frac{\sigma^2}{1 + d\left(\chi^2 + \psi^2\right)} \begin{bmatrix} \left(1 + d\chi^2\right)^2 & (d\chi\psi)^2 \\ (d\chi\psi)^2 & \left(1 + d\psi^2\right)^2 \end{bmatrix},$$

where σ^2 is the variance of the measurement errors associated with χ and ψ, and d is on the order of 1.

The focal length is assumed to be unitary and the sensor boresight is assumed to be the z-axis. Hence, the measurement vector in the object space and sensor frame is given by

$${}^s\mathbf{d} = \frac{1}{\sqrt{1 + \chi^2 + \psi^2}} \begin{bmatrix} \chi \\ \psi \\ 1 \end{bmatrix}.$$

B. Closeness metrics

The configuration closeness to the degenerate case (6) is evaluated by the metric given by $\tau_1 = \left| \left(\|\mathbf{d}_1^T \mathbf{d}_{1/2}\| \right) - 1 \right|$. For the ambiguous case consider the metric given by $\tau_2 = \mathbf{d}_{1/2}\mathbf{R}\left(\alpha, \mathbf{d}_1\right) \frac{\mathbf{S}(\mathbf{d}_1)\mathbf{d}_{1/3}}{\|\mathbf{S}(\mathbf{d}_1)\mathbf{d}_{1/3}\|}$, where α is obtained from (7).

In both τ_1 and τ_2, the closer these metrics are to zero the closer the configurations are to the respective special case.

C. Simulation setup

In both cases, there is a set of 40 different configurations in an interval of 10 seconds, following a specific transformation of the initial configuration. Each configuration is simulated for 1000 Monte Carlo trials, in which measurements are taken, following the sensor model just described with standard deviation $\sigma = 17 \times 10^{-6}$, the same from problems with similar sensors [10], and then applying the solution algorithm from [13]. Furthermore, for simplicity, the sensor boresight axes are assumed to be aligned with the measurement that they are taking.

1) Initial Configuration: The initial configuration is the same in both cases, it has a unique solution, and it is given by

$$\mathbf{R}_1^I = \begin{bmatrix} \cos\frac{\pi}{6} & -\sin\frac{\pi}{6} & 0 \\ \sin\frac{\pi}{6} & \cos\frac{\pi}{6} & 0 \\ 0 & 0 & 1 \end{bmatrix},$$

$$\mathbf{R}_2^1 = \begin{bmatrix} \cos\frac{\pi}{3} & 0 & -\sin\frac{\pi}{3} \\ 0 & 1 & 0 \\ \sin\frac{\pi}{3} & 0 & \cos\frac{\pi}{3} \end{bmatrix},$$

$$\mathbf{R}_3^1 = \begin{bmatrix} 1 & 0 & 0 \\ 0 & \cos\frac{\pi}{4} & \sin\frac{\pi}{4} \\ 0 & -\sin\frac{\pi}{4} & \cos\frac{\pi}{4} \end{bmatrix},$$

$${}^I\mathbf{d}_1 = \begin{bmatrix} 0 & 0 & 1 \end{bmatrix}^T,$$

$${}^I\mathbf{d}_2 = {}^I\mathbf{d}_3 = \begin{bmatrix} \sin\frac{\pi}{6} & \cos\frac{\pi}{6} & 0 \end{bmatrix}^T,$$

$${}^I\mathbf{d}_{1/2} = \mathbf{R}_1^I \mathbf{d}_{1/2} = \begin{bmatrix} 1 & 0 & 0 \end{bmatrix}^T,$$

and $${}^I\mathbf{d}_{1/3} = \mathbf{R}_1^I \mathbf{d}_{1/3} = \begin{bmatrix} -\sin\frac{\pi}{6} & \cos\frac{\pi}{6} & 0 \end{bmatrix}^T.$$

2) Degenerate case: In this case, ${}^I\mathbf{d}_{1/3}$ is incrementally rotated by $\frac{\pi}{120}$ rad about the axis given by $[0\ 0\ 1]^T$, such that in total it rotates $\frac{\pi}{3}$ rad and the final value of this parameter is $\left({}^I\mathbf{d}_{1/3}\right)_f = \begin{bmatrix} \sin\frac{\pi}{6} & \cos\frac{\pi}{6} & 0 \end{bmatrix}^T = {}^I\mathbf{d}_3$. Notice that this transformation affects both $\mathbf{d}_{1/3}$ and $\mathbf{d}_{3/1}$.

3) Ambiguous case: In this case, ${}^I\mathbf{d}_3$ is incrementally rotated by $\frac{\pi}{120}$ rad about the axis given by $[0\ 0\ 1]^T$, such that in total it rotates for a total of $\frac{\pi}{3}$ and the final value of this parameter is $\left({}^I\mathbf{d}_3\right)_f = \begin{bmatrix} -\sin\frac{\pi}{6} & \cos\frac{\pi}{6} & 0 \end{bmatrix}^T$.

D. Results

The results are given by the plot of the standard deviation of each Euler angle error for each configuration tested. Moreover, the corresponding metric is plotted, so that both values can be analyzed together. First, the results for the degenerate case are shown in Figs. 7, 8, and 9 respectively for the errors of $\mathbf{R}_2^1$, $\mathbf{R}_3^1$, and $\mathbf{R}_1^I$. Analyzing Fig. 8, the deterioration of the accuracy, which results from the proximity to the degenerate configuration, is visible in the last seconds of the roll and the pitch standard deviations. Notice that the scale of representation in this figure is logarithmic, therefore, the error increases significantly in the final seconds, before a point, when it is practically a degenerate configuration and the solution diverges. The attitude determination of $\mathbf{R}_2^1$ and $\mathbf{R}_1^I$ are not affected by this degenerate case because in the case of $\mathbf{R}_2^1$, there is no dependency on $\mathbf{R}_3^1$. In the case of $\mathbf{R}_1^I$, the averaging of both candidates offsets this error.

The ambiguous case results are shown in Figs. 10, 11, and 12. The main observation here is the fact that the standard deviation for $\mathbf{R}_2^1$, $\mathbf{R}_3^1$, and $\mathbf{R}_1^I$, suddenly diverge when the configuration is close enough to the ambiguous case. Notice that the standard deviation of the yaw angle is in logarithmic scale in both figures. In the last configuration, when $\tau_2 \approx 0$, the results of the algorithm alternate between the two ambiguous solutions and the corresponding standard deviation increases a lot, because the error of one of the solutions is very large.

V. CONCLUSIONS

In this paper, the special cases for the three-vehicle formation attitude determination problem were described. In these cases, the solution is not unique and there are either infinite or two solutions, denoted as degenerate or ambiguous configurations accordingly. An important property of the set of special configurations is a zero measure subset of the entire subset of configurations. Hence, the problem can be applied in a real world scenario. Two simulations were carried out to show that the algorithm cannot give the correct solution, when the configurations are close to this specific cases. In the degenerate case simulation, the standard deviation increases slightly, after a certain threshold, as the configuration gets closer the degenerate one, until the moment when it diverges. In the ambiguous case simulation, the standard deviation suddenly diverges, when the configuration is close enough to the ambiguous case for the noise to impact the outcome of the algorithm. Both results correspond to the expected behavior of the respective case.

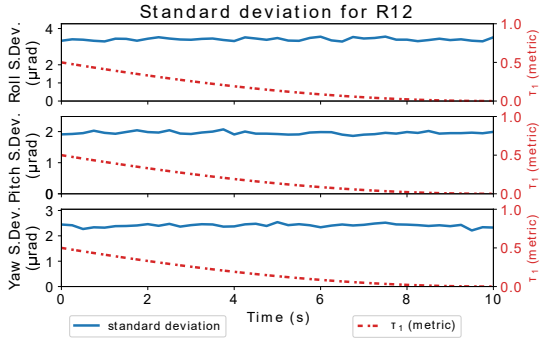

Fig. 7. Standard deviations of $\mathbf{R}_2^1$ error in degenerate case.

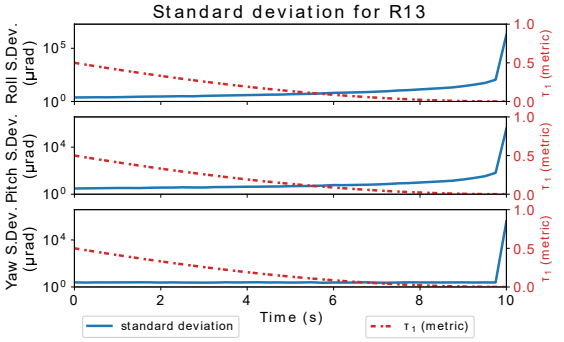

Fig. 8. Standard deviations of $\mathbf{R}_3^1$ error in degenerate case.

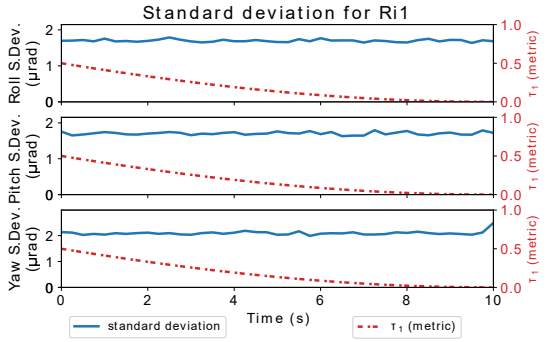

Fig. 9. Standard deviations of $\mathbf{R}_1^I$ error in degenerate case.

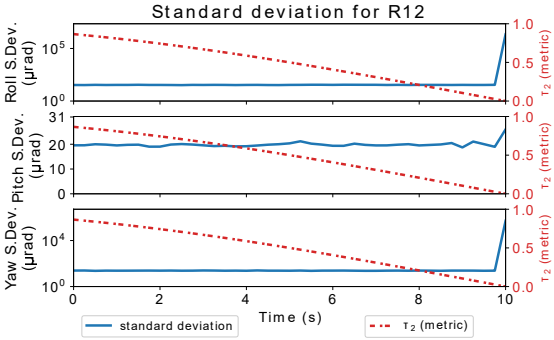

Fig. 10. Standard deviations of $\mathbf{R}_2^1$ error in ambiguous case.

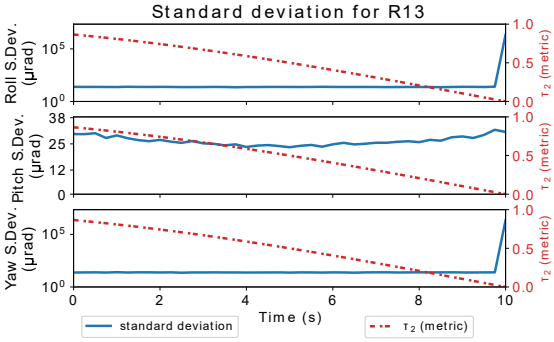

Fig. 11. Standard deviations of $\mathbf{R}_3^1$ error in ambiguous case.

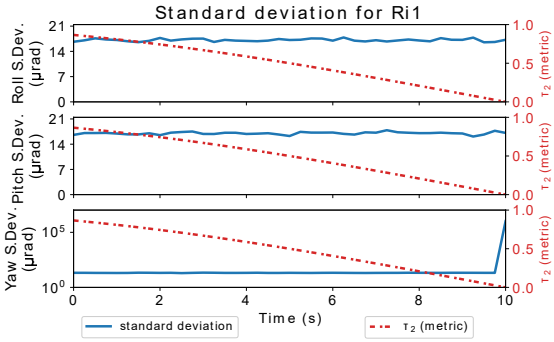

Fig. 12. Standard deviations of $\mathbf{R}_1^I$ error in ambiguous case.

REFERENCES

[1] H. Black, "A passive system for determining the attitude of a satellite," *AIAA Journal*, vol. 2, no. 7, pp. 1350–1351, July 1964.

[2] G. Wahba, "A least-squares estimate of satellite attitude," *SIAM Review*, vol. 7, no. 3, p. 409, July 1965.

[3] P. B. Davenport, "Vector approach for the algebra of rotations with applications," NASA-TN-D-4696, Tech. Rep., 1965.

[4] M. D. Shuster and S. D. Oh, "Three-axis attitude determination from vector observations," *Journal of Guidance, Control and Dynamics*, vol. 4, pp. 70–77, Jan. 1981.

[5] L. Markley, "Attitude determination using vector observations and the singular value decomposition," *Journal of the Astronautical Sciences*, vol. 36, no. 3, pp. 245–258, Nov. 1987.

[6] J. Wu, Z. Zhou, B. Gao, R. Li, Y. Cheng, and H. Fourati, "Fast linear quaternion attitude estimator using vector observations," *IEEE Transactions on Automation Science and Engineering*, vol. 15, no. 1, pp. 307–319, Jan 2018.

[7] F. L. Markley and J. L. Crassidis, *Fundamentals of Spacecraft Attitude Determination and Control*, 1st ed. New York: Microcosm Press and Springer, 2014.

[8] D. P. Scharf, F. Y. Hadaegh, and S. R. Ploen, "A survey of spacecraft formation flying guidance and control (part 1): guidance," in *Proceedings of the 2003 American Control Conference, 2003.*, vol. 2, June 2003, pp. 1733–1739.

[9] Y. Cao, A. Fukunaga, and A. Kahng, "Cooperative mobile robotics: Antecedents and directions," *Autonomous Robots*, vol. 4, pp. 7–27, 1997.

[10] R. Linares, J. L. Crassidis, and Y. Cheng, "Constrained relative attitude determination for two-vehicle formations," *Journal of Guidance, Control and Dynamics*, vol. 34, no. 2, pp. 543–553, Mar. 2011.

[11] X. S. Zhou and S. I. Roumeliotis, "Determining 3-d relative transformations for any combination of range and bearing measurements," *IEEE Transactions on Robotics*, vol. 29, no. 2, pp. 458–474, 2013.

[12] R. Cesarone, D. Abraham, and L. Deutsch, "Prospects for a next-generation deep-space network," *Proceedings of the IEEE*, vol. 95, pp. 1902 – 1915, 11 2007.

[13] P. Cruz and P. Batista, "A solution for the attitude determination of three-vehicle heterogeneous formations," *Aerospace Science and Technology*, vol. 93, p. 105275, 2019. [Online]. Available: http://www.sciencedirect.com/science/article/pii/S1270963817322071

[14] M. D. Shuster and S. D. Oh, "Three-axis attitude determination from vector observations," *Journal of Guidance, Control and Dynamics*, vol. 4, pp. 70–77, Jan. 1981.

[15] M. D. Shuster, "Kalman filtering of spacecraft attitude and the quest model," *The Journal of the Astronautical Sciences*, vol. 38, no. 3, pp. 377–393, Sept. 1990.